Paper AAS 06-196

MULTI-OBJECTIVE PARALLEL GENETIC ALGORITHMS APPLIED TO THE PRIMER VECTOR CONTROL LAW

Seungwon Lee
Ryan P. Russell

Jet Propulsion Laboratory
Californian Institute of Technology
4800 Oak Grove Dr. Pasadena, CA

16th AAS/AIAA Space Flight Mechanics Conference

Tampa, Florida **January 22-26, 2006**

AAS Publications Office, P.O. Box 28130, San Diego, CA 92198

AAS 06-196

MULTI-OBJECTIVE PARALLEL GENETIC ALGORITHMS APPLIED TO THE PRIMER VECTOR CONTROL LAW

Seungwon Lee[1] and Ryan P. Russell[2]

A global, Pareto, and parallel optimization method for low-thrust orbit transfers is developed by applying a multi-objective parallel genetic algorithm to the Primer Vector control law. Complex trajectories are parameterized with the well-known Primer Vector control law using only the initial values of a co-state vector. The multi-objective parallel genetic algorithm searches for initial values that lead to mass- and time-optimal trajectories that satisfy a prescribed final target condition. The optimization method yields a set of Pareto-optimal solutions, which demonstrate the trade-off between ΔV and flight time for a given low-thrust orbit transfer. The method is applied to three different multiple-revolution orbit transfer problems: 1) a two-body orbit transfer around the Earth, 2) a restricted three-body, coplanar distant retrograde orbit (DRO) transfer around Europa, and 3) a restricted three-body, non-coplanar DRO transfer around Europa. The resulting Pareto-optimal solutions are comparable to those from state-of-the-art optimization tools such as Mystic and GA-Q-Law.

INTRODUCTION

NASA's Deep Space 1 mission has demonstrated that a low-thrust propulsion system can reliably operate for a long period of time with a low cost of propellant thanks to its high specific impulse. As low-thrust propulsion systems are now a proven technology, a host of future missions are considering this efficient alternative to reduce mission cost and increase final payload mass. A low-thrust propulsion system requires a longer period of thrusting than a chemical propulsion system in order to accelerate a spacecraft to the same final velocity. Therefore, the low-thrust trajectory involves a continuously changing thrust profile as opposed to the impulsive maneuvers found in a traditional high-thrust trajectory. It is the complex thrusting profile that makes the design of optimal low-thrust trajectories very challenging.

Various methodologies have been applied to the optimization of low-thrust trajectories. Broadly speaking, there are three philosophically different approaches for trajectory optimization as for optimization problems in general. They are 1) deterministic optimization, 2) probabilistic optimization, and 3) control strategy development.

[1] Member of the Information and Computer Science Staff at Jet Propulsion Laboratory, California Institute of Technology, Pasadena, CA. Email: Seungwon.Lee@jpl.nasa.gov.

[2] Member of the Engineering Staff at Jet Propulsion Laboratory, California Institute of Technology, Pasadena, CA. Email: Ryan.Russell@jpl.nasa.gov.

Deterministic optimization utilizes numerical optimal control methods that are based on principles such as the calculus of variations, nonlinear programming methods, neighboring extremal methods, and gradient-based methods [1-6]. These methods are deterministic because for a given initial guess the final result is always identical in every run. In contrast, probabilistic optimization utilizes randomness in the search process. Some examples are Monte Carlo algorithms, evolutionary algorithms, simulated annealing, and cultural programming [7-10]. Finally, control strategy development aims at finding efficient control laws that indirectly yield optimal or near- optimal solutions. The feedback control laws can be designed as stand-alone tools or wrapped by optimizers such as evolutionary algorithms and evolving neural networks [11-17].

Each of these approaches emphasizes different aspects of the optimization. The deterministic optimization approach tends to be a local optimizer because it uses first- or second-order derivatives (i.e. local environment) of one potential solution to update the solution in iterations. The probabilistic optimization approach is designed to be a global optimizer by replacing the local-environment feedback with the global-environment feedback. Examples include statistical sampling in Monte Carlo method, reproduction mechanisms in evolutionary algorithms, Metropolis algorithms in simulated annealing, and swarm intelligence principles in Particle Swarm Optimization. The control strategy development approach finds the common rule that can be applied to a suite of trajectories. Thus, it is more efficient and general but not necessarily optimal for a particular trajectory.

The paper presents a hybrid method that combines the control strategy and probabilistic methods. The control component of the hybrid method is the Primer Vector control law [3-6]. This is a feedback law for determining the thrust vector and is a function of the current co-state only. It implicitly satisfies optimality conditions with regard to the thrust magnitude and direction. The probabilistic part is a multi-objective genetic algorithm [18-20] that directly optimizes the initial co-state vector to minimizes the propellant mass and the flight time for a given low-thrust orbit transfer problem.

This hybrid approach is particularly attractive because it avoids one of the problems typically associated with indirect methods: i.e. gradients and transversality conditions must be tediously re-derived each time an objective or constraint is changed. The transversality conditions are implicitly satisfied by directly optimizing the initial co-states, and the gradients are not required for the current genetic optimization methods. Therefore, the problem can be tailored for custom applications with relative ease compared to traditional methods.

The application of genetic/evolutionary algorithms to trajectory optimization has recently gained popularity and is shown to be efficient in generating globally optimal solutions and initial guess values for subsequent refinement and local optimization. Just to name a few, a multi-objective genetic algorithm is used to optimize the control parameters of Lyapunov feedback control law named Q-law for low-thrust two-body

orbit transfers [15-17], a combination of evolution programming and branching is used to optimize interplanetary trajectories [21], a combination of multi-objective genetic algorithm and nonlinear programming is applied to optimize orbit escape and capture and interplanetary transfer [22], a genetic algorithm is applied to optimize low-thrust Earth-Mars trajectories [23], impulsive maneuvers and gravity assists in deep-space interplanetary trajectories are optimized using a genetic algorithm [24], and optimal continuous thrust orbit transfers are found using evolutionary strategies [25].

In this paper, the structure of the developed hybrid method is described and is followed by the application of the hybrid method to three multiple-revolution low-thrust trajectory optimization problems that include two-body orbit transfers and three-body orbit transfers. The optimization results are presented in terms of Pareto fronts and corresponding trajectories. In two of the cases, the optimization performance of the hybrid method is compared with other state-of-the-art optimizing methods. This paper complements and expands upon the research that is overviewed in Refs. [26,27].

APPROACHES

Primer Vector Control Law

The Primer Vector control law is a well known result of the application of calculus of variations to the low-thrust spacecraft problem. See Refs. [3-6] for detailed equations, derivations, and applications. The Primer Vector theory introduces a co-state vector and "indirectly" optimizes the thrust control variables by adjusting the initial values of the co-state vector. This method uses the optimality conditions (Euler-Lagrange equations) that arise from calculus of variations to transform the control vector into a function of the current co-states only. Traditionally, this transformation combined with the Euler-Lagrange boundary conditions, or the so-called transversality conditions, leads to a two-point boundary-value problem, whose solution inherently satisfies the necessary conditions for local optimality. In the current approach, any applicable transversality conditions are ignored, and the initial values of the co-states are iterated to directly optimize the desired objective.

The spacecraft state and co-state equations are propagated and the thrusting magnitude and direction at all times satisfy the necessary conditions for optimality. This consists of thrusting with a maximum thrust in the direction of the Primer Vector when the prescribed switching function is positive and turning off thrust when the switching function is negative. To avoid discontinuities in the equations of motion, the propagation is interpolated to stop exactly when the switching function changes sign. In this manner the integration is cycled through a series of "bang-bang" maneuvers with no limit or preconceived notion of number of switches. The integration is stopped when some maximum time is achieved or a user defined stopping condition is met.

An adjoint control transformation is applied to the initial conditions to map

physically meaningful control variables to the more abstract initial co-states that are required to implement the Primer Vector theory. The six alternative initial co-state values named alpha, alpha dot, beta, beta dot, switching function, and switching function dot are related to thrust angles and thrust on/off conditions. Alpha controls the thrust angle defined in the orbit plane perpendicular to the angular momentum, and alpha dot is the time derivative of the thrust angle. Similarly, beta controls the thrust angle off the orbit plane, and beta dot controls the time derivative of the angle. Both alpha and beta are orientation angles expressed in a reference frame that aligns its x axis with the spacecraft velocity and its z axis with its angular momentum. Finally, the switching function and its time derivative (switching function dot) helps in determining the initial frequency of switching times, i.e. when to thrust or coast. Remarkably, with the six variables, a complicated trajectory can be uniquely defined and controlled. The orbit propagator implemented in this study including the adjoint control transformation is described in detail in Ref. [6]

Multi-objective Parallel Genetic Algorithm

A genetic algorithm is tuned to efficiently solve the optimization problem formulated within the Primer Vector control law. While following the basic procedure of the genetic algorithms, several special features are added in the ranking/fitness-assignment process. The key aspects of the refined genetic algorithm are described below: 1) stochastic ranking, 2) non-dominated sorting, 3) fitness sharing, 4) parallel computing.

Stochastic Ranking: Our optimization problem is constrained and has multiple objectives. Meeting the constraints and improving the objectives are often competing tasks. Typically, the constraints are treated with a penalty function, and the penalty function and the objective function are combined into a single scalar fitness function with associated weights. In this scheme, the optimization direction and outcome are sensitive to the weights and thus choosing the right weights becomes a critical step in the optimization process. To avoid the sensitivity, we use stochastic ranking to maneuver the balance between the two tasks [28]. In the stochastic ranking process, the ranking criterion is probabilistically chosen between the constraint-based and objective-based one. Typically, slightly more emphasis on the constraint-based ranking (55%) over the objective-based ranking (45%) shows the best performance. The stochastic ranking also involves the user-specified parameter that determines the probability to choose one ranking criterion over the other. However, the parameter has a more straightforward meaning to the balancing between the two tasks (meeting the constraints and improving the objectives). Hence, it is easier to control the sensitivity of the optimization problem to the user-specified parameter.

Non-dominated Sorting: When multiple competing objectives are involved, improving one objective is often accompanied by degrading other objectives. Hence, the multi-objective problem gives rise to a set of compromising solutions rather than a single

optimal solution. The multi-objective aspect of our optimization process is steered by non-dominated sorting, where solutions are evaluated according to the Pareto-dominance concept [20]. When comparing two solutions, a solution is termed "Pareto-dominated" if the solution is inferior to the other solution in all objectives. Otherwise, the solution is termed "non-Pareto-dominated". The principle of the multi-objective optimization is to reward "non-Pareto-dominated" solutions over "Pareto-dominated" solutions. In the non-dominated sorting, first non-Pareto-dominated solutions in the population are selected, and they form a first Pareto front. The same selection process is performed for the remainder of the population excluding the first Pareto front, and the non-Pareto-dominated solutions form a second Pareto front. This process repeats until all the members of the population are assigned to a Pareto front. A different fitness value is assigned to each Pareto front. The first Pareto front is most rewarded in terms of fitness value, and so on.

Fitness Sharing: The search space of our optimization problem typically contains tiny and disjointed feasible spaces (solutions that meet constraints) and even tinier optimal spaces (Pareto-optimal solutions). In such a search space, a few feasible/sub-optimal solutions can easily dominate the search direction. To prevent the domination by a few good initial solutions and hence to obtain an extended Pareto front, a fitness sharing mechanism is applied [7]. In our application, solutions are divided into a prescribed number of groups according to their flight times. Each group has the maximum and minimum flight times allowed. Within the group, the fitness values of all the solutions are summed and the fitness value of each solution is normalized by the sum. The normalization process makes the total fitness value of each group to be one. Therefore, each group has an equal possibility to survive and create offspring. This mechanism encourages diversity among solutions in terms of flight times.

Parallel Computing: Parallel computing is incorporated into the genetic algorithm process in order to accelerate computation. The fitness evaluation in the genetic algorithm process is highly independent and therefore is easily distributed among multiple processors in a distributed-memory system. The fitness value is the only message passing between the processors. As a result, the computational overhead due to the parallel computing is marginal, and the computation speedup is close to ideal.

Hybrid Method

The Primer Vector control law and the multi-objective parallel genetic algorithm are coupled to generate Pareto-optimal trajectories for a given problem. In the hybrid method, the Primer Vector control law implicitly satisfies the Euler-Lagrange equations. However, the resulting trajectories do not necessarily satisfy the natural boundary conditions (transversality conditions) nor the terminal condition given by the target state. It is the task of the multi-objective parallel genetic algorithm to find trajectories that satisfy the boundary conditions and are globally Pareto-optimal solutions. While the traditional

boundary value problem only satisfies necessary conditions for optimality, the hybrid optimizer employed in this study also approximates the sufficiency conditions because it guarantees descent. Furthermore, it seeks global minima while the boundary value problem applies to local solutions only. The overall optimization procedure of the hybrid method is described in Figure 1.

1. Randomly populate the initial co-state vector and flight time.
2. Propagate trajectories with the co-state vector and flight time using the Primer Vector control law. This step is run on multiple processors in parallel.
3. Evaluate the trajectories based on the used propellant mass, the flight time, and the error of the final state to the target state.
    a. Rank the trajectories using the non-dominated sorting (Rank I).
    b. Rank the trajectories according to constraint violation degree (Rank II).
    c. Mix the Rank I and II using stochastic ranking (Rank III).
        i. For 45% of comparisons, use Rank I result.
        ii. For 55% of comparisons, use Rank II result.
    d. Use Rank III as the fitness value of each trajectory.
    e. Share the fitness value among the solutions at each flight time zone.
4. Choose parent co-state vector using binary tournament.
5. Create offspring co-state vector using crossover and mutation operations to parents.
6. Increment the generation number by one.
7. Go to Step 2 until the maximum generation number is reached.
8. Final results are constraint-satisfied (to a specified tolerance) and Pareto-optimal solutions.

Figure 1. Overall procedure of the hybrid method.

ORBIT TRANSFER PROBLEMS

Three problems are formulated to test the present method. Each problem has a different complexity degree and is governed by one of two different dynamical models. The first problem is a coplanar two-body orbit transfer around the Earth. Since it is a coplanar transfer, it does not involve thrust along the angular momentum direction, leading the optimization to only four initial co-state values (alpha, alpha dot, switching function, and switching function dot). The second problem is a coplanar, restricted three-body, distant retrograde orbit (DRO) transfer around Europa. This problem is slightly more complex than the first one due to the three-body orbit dynamics involving Jupiter's gravity. The third problem is a non-coplanar, restricted three-body, DRO transfer around Europa. This problem is most complex since it involves multi-body effects and thrust both in and out of the orbit plane. The three problems are labeled Problem I, Problem II, and Problem III, respectively. The details of the orbit parameters of the problems are listed in Table I, II, and III.

Table 1: Problem I – Initial and target orbit elements, thrust characteristics, and spacecraft initial

mass for the two-body orbit transfer around the Earth. The orbit elements are given by the semi-major axis (a), the eccentricity (e), the inclination (i), the argument of the periapsis (ω)), , the longitude of the ascending node (Ω).

Orbit	a (km)	e	i (degrees)	ω (degrees)	Ω (degrees)	Thrust (N)	Specific Impulse (s)	Initial Mass (kg)
Initial	9222.7	0.2	0.573	0.0	0.0	9.3	3100	300
Target	30000.0	0.7	Free	Free	Free			

Table 2: Problem II – Initial and target states, thrust characteristics, and spacecraft initial mass for the restricted three-body, coplanar, distant retrograde orbit transfer around Europa. The initial and target states are given by the position and velocity vector in the rotating frame where Europa is at the center, the x-axis points along the Jupiter-Europa line, and the z-axis points along the system angular momentum vector.

State	x (km)	y (km)	z (km)	v_x (km/s)	v_y (km/s)	v_z (km/s)	Thrust (N)	Specific Impulse (s)	Initial Mass (kg)
Initial	50,445	0	0	0	-2.0600	0	4.98	7365	25000
Target	20,579	0	0	0	-0.9995	0			

Table 3: Problem III – Initial and target states, thrust characteristics, and spacecraft initial mass for the restricted three-body, non-coplanar, distant retrograde orbit transfer around Europa. The initial state is given by the position and velocity vector in the rotating frame where Europa is at the center, the x-axis points along the Jupiter-Europa line, and the z-axis points along the system angular momentum vector. The target state is given by the orbit elements: semi-major axis, eccentricity, inclination for the orbit defined by the Europa gravity only.

Initial	x (km)	y (km)	z (km)	v_x (km/s)	v_y (km/s)	v_z (km/s)	Thrust (N)	Specific Impulse (s)	Initial Mass (kg)
	20,579	0	0	0	-0.9995	0			
Target	Semimajor axis (km)		eccentricity		inclination (deg.)		4.98	7365	25000
	[7000, 9000]		[0.0, 0.2]		[130, 140]				

OPTIMIZATION RESULTS

Problem I: two-body coplanar orbit transfer around the Earth

In this problem, the Earth is the only gravitational body and is approximated as a point mass. Figure 2 shows the Pareto-optimal solutions found with the present methods. The Pareto-optimal solutions have one percent of error tolerances between the computed final orbit and the given target orbit. The present solutions are compared with the solutions found with GA-Q-Law, which is an optimized heuristic control law based on a Lyapunov feedback control law named Q-law and a genetic algorithm [11-17]. It has been demonstrated that the GA-Q-Law finds a Pareto front of near-optimal solutions in a reasonable computation time. The present method efficiently yields solutions comparable to GA-Q-law solutions for a wide range of flight times. Note that GA-Q-law solutions (error<0.03%) have a much lower error tolerance than the present solutions.

Figure 3 shows eight Pareto-optimal trajectories selected among the Pareto-optimal solutions found with the present method. As the flight time increases, several coast (no-thrust) arcs (green dashed lines) are inserted around the apoapsis. These variations demonstrate how propellant is saved with the expense of flight time in this transfer. As expected, thrust around the periapsis is more propellant efficient than other places and the present method captures the efficient thrust mechanism.

Problem II: restricted three-body, coplanar DRO transfer in Jupiter-Europa system

This problem is a restricted three-body, coplanar DRO transfer around Europa, the icy Galilean moon closest to Jupiter. The gravitational fields of Jupiter and Europa are included as point masses, while the gravitational fields of the other moons are excluded. The dynamics of the spacecraft are described in the rotating frame where Europa is at the center, the x-axis points along the Jupiter-Europa line, and the z-axis points along Europa's angular momentum vector with respect to Jupiter.

Figure 4 shows the Pareto-optimal solutions obtained with the present method in comparison with the solutions obtained with Mystic, a high-fidelity trajectory optimization software package based on the static/dynamic control algorithm [29,30]. The solutions with the present method have one percent of error tolerances between the final state and the given target state. Specifically, the final position has the error of up to 206 km in x and y values and the final velocity has the error of up to 0.01 km/s. Mystic solutions have a tighter error tolerance which is below 0.1 percent. Because Mystic utilizes local gradients in finding optimal solutions, the refinement of the solutions at the final state is relatively easier than the present method where no local gradients are used. The present method is not suited to refine the solutions up to the error level of Mystic solutions. Due to the difference in the error tolerance level, Mystic solutions have a higher

Delta V or a longer flight time than our solutions.

This six-state to six-state transfer leads to a disjointed Pareto front with no Pareto-optimal solution in some range of flight times. This does not mean that there is no feasible trajectory in some flight times. The disjointed Pareto front represents that for a certain range of flight time the increase of the flight time does not lead to the saving of propellant. This situation is attributed to our target state that is one particular location on a DRO instead of a phase-free location on a given DRO. This concept is highlighted by comparing the results to those presented in Ref. [6] where the same problem is solved except the target DRO orbit is phase-free.

Figure 5 shows the variations of the trajectory and control profile for a few selected Pareto-optimal solutions. As the flight time increases, more and wider coast arcs (green dashed lines) are inserted around the y-axis. This shows that thrust around the y-axis is propellant efficient for this transfer.

Problem III: restricted three-body, non-coplanar, phase-free DRO transfer in Jupiter-Europa system

This problem is a restricted three-body, non-coplanar DRO transfer around Europa, involving about 40 degrees of inclination change. The initial state of this problem is given by a six-state vector, while the target state is given by three orbit elements (semi-major axis, eccentricity, and inclination) of the orbit defined by the Europa gravity only. The target orbit elements fluctuate in time, but are relatively stable for over 100 Earth days. Considering the fluctuation of the target orbit elements, our target conditions are loose and given by the range of the temporal variation of the orbit element, as listed in Table III. Because this transfer involves a large inclination change, all six initial co-state variables including beta and beta dot are optimized in contrast to the previous two problems.

We have performed 10 independent optimization runs with different random seeds and genetic-algorithmic parameters such as population size and reproduction operators. The best Pareto front is found with an optimization run using the population size of 10,000 and the maximum generation number of 400. Figure 6 plots the result of the best optimization run. The figure shows the progress of the Pareto fronts as the optimization process proceeds. The Pareto front becomes more optimal and wider as more generations (iterations in the genetic algorithm) are processed. The final Pareto front is disjointed. This implies either the absence of Pareto-optimal solutions in some flight times or the failure of finding Pareto-optimal solutions with the present method. More independent optimization runs are needed to identify the cause.

Figure 7 shows the dynamics of the orbit element for two boundary solutions (the shortest and longest flight-time solutions) of the Pareto front at generation 400. One reaches the target DRO after 26.0 days and the other after 28.2 days. After reaching the target, the trajectories are propagated for additional 40 days without thrust to monitor the stability of the final orbit. Both trajectories remain stable as intended.

The stability of a DRO is closely related to its out-of-plane motion and its proximity to the central body. Accordingly, Figure 8 is a surface plot of the time until impact or escape for a DRO around Europa with specified initial inclination and close approach distance [31]. The DROs generally enjoy a peninsula of stability when they are close to Europa and have inclinations above 135 degrees. The initial and final target orbits for Problem III were intentionally selected to be near the stability boundary. To examine the intermediate stability of the two Pareto front solutions, the discreet close approach points on each trajectory are plotted on top of the stability map. In both cases, the trajectories meander into the unstable region where small perturbations to the control can have large affects on the orbit. This is expected for orbits that seek to minimize fuel expenditures because thrusting is more efficient in the unstable regions. Since the Pareto optimal solutions also seek to minimize time, the paths of the solutions are generally straight, which keeps them near the stable regions. If fuel is the only objective, the optimal trajectories will likely take a less direct approach through the regions of greater instability [31,32]. The paths of both trajectories are consistent with the expected optimal path.

The top view (x-y plane) and side view (x-z plane) of the two trajectories in the rotating frame centered at Europa are plotted in Figure 9. The thrust profiles of the two solutions are described in Figures 10 and 11 in terms of thrust angles and magnitudes, respectively. The thrust angle is defined by the relative angle between the thrust vector and the spacecraft velocity vector in the rotating frame. Initially, in order to optimally change the inclination, the thrust vector is perpendicular to the velocity when the spacecraft is near Europa's orbit plane. Towards the end of the trajectory, the thrust vector generally points against the velocity vector to reduce the semi-major axis. The plot of the thrust magnitudes in Figure 11 shows the bang-bang maneuvers structure of the Primer Vector control law. Note there are multiple coast arcs in each trajectory. The solution with the flight time of 26 days has very short coast arcs, indicating that it is close to the shortest flight time solution.

CONCLUSIONS

We have demonstrated a new method to obtain Pareto-optimal solutions for low-thrust orbit transfers for both two-body and three-body problems. The method combines the Primer Vector control law and the multi-objective parallel genetic algorithm, where the Primer Vector control law generates a thrust profile for a given initial value of a co-state vector and the multi-objective parallel genetic algorithm finds the initial value that both satisfies the target state's boundary condition and minimizes ΔV(or propellant mass) and flight time. The optimization method yields in a single run a set of Pareto-optimal solutions, which demonstrates the trade-off between ΔV and flight time for a given low-thrust orbit transfer. The method is successfully applied to three orbit transfer problems and the resulting Pareto-optimal solutions are comparable to those from state-of-the-art

optimization tools such as Mystic and GA-Q-Law.

The method is computationally efficient and requires relatively low domain expertise. The only initial requirement of the optimization process is a reasonable bound on each variable and a single synergistic optimization run leads to Pareto-optimal solutions. The method efficiently finds the optimal solutions within a reasonable error threshold. However, for a tighter error threshold, it is more desirable to delegate the refinement of the final solutions to a local gradient-based algorithm. The method is best suited for the rapid feasibility check and trade-space exploration in a low-fidelity mission design.

ACHKNOWLEDGEMENTS

The authors acknowledge the contributions and support from Anastassios Petropoulos, Richard Terrile, Paul von Allmen, Wolfgang Fink, and Jon Sims. This work was carried out at the Jet Propulsion Laboratory, California Institute of Technology, under a contract with the National Aeronautics and Space Administration. The research was supported by the JPL's Research and Technology Development program.

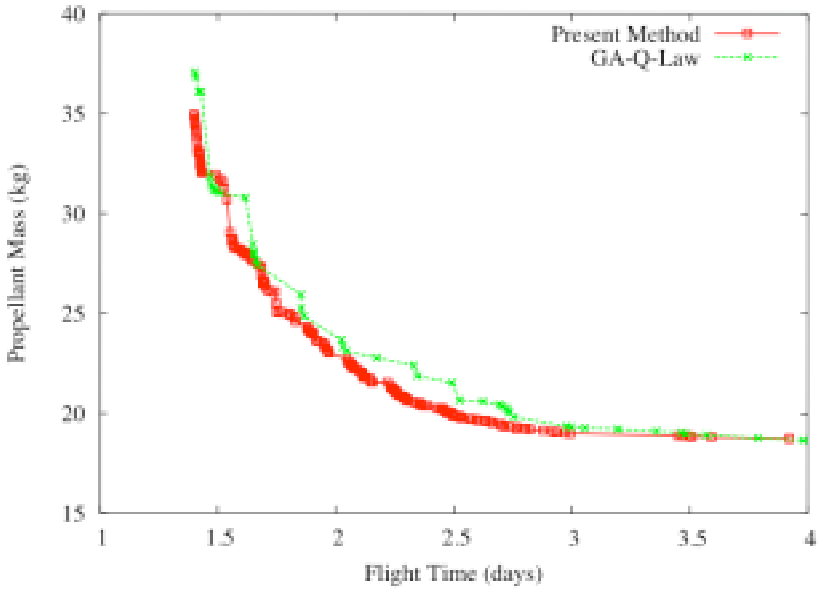

Figure 2. Pareto-optimal solutions found with the present method in comparison with GA-Q-Law solutions for Problem I. The error tolerance between the final and target orbit is 1% and 0.03% for the present method and GA-Q-Law solutions, respectively. Since the GA-Q-Law error tolerance is lower, the present method estimates a lower propellant-mass budget than GA-Q-Law.

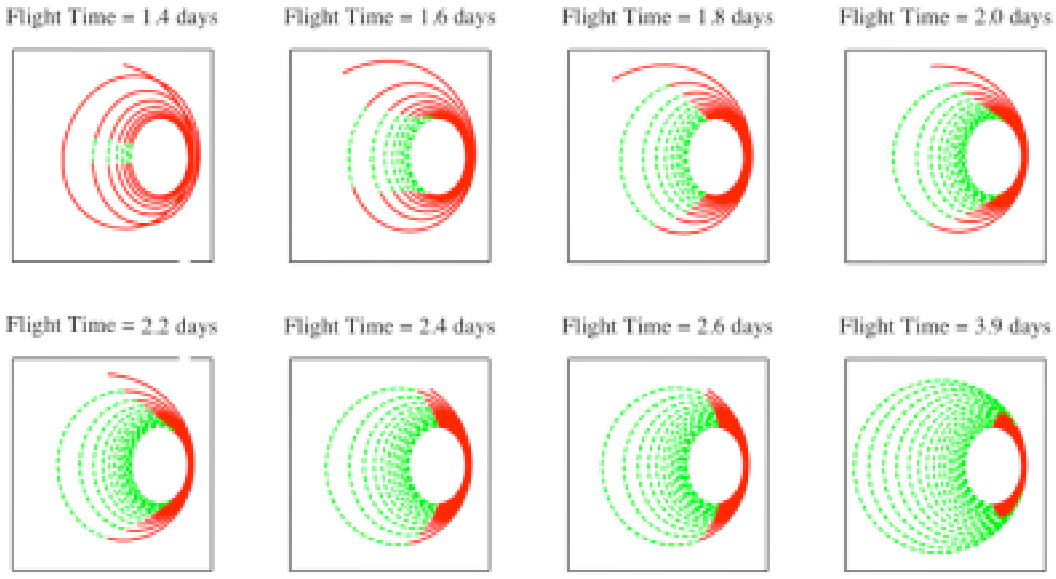

Figure 3. Pareto-optimal trajectories found with the present method for Problem I. The red solid and the green dashed lines represent thrusting and coasting arcs, respectively. As the flight time increases, several coast arcs are inserted around the apoapsis.

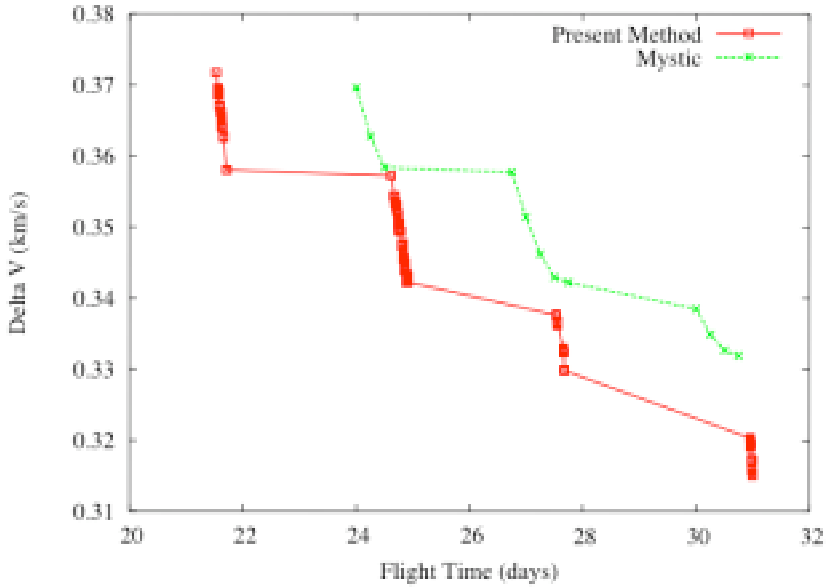

Figure 4. Pareto-optimal solutions found with the present method in comparison with Mystic solutions for Problem II. The error tolerance between the final and target orbit is 1% and 0.1% for the present method and Mystic solutions, respectively. Since the Mystic error tolerance is ten times lower, the present method estimates a lower Delta V budget than Mystic. The general trends of the two solution sets are very similar.

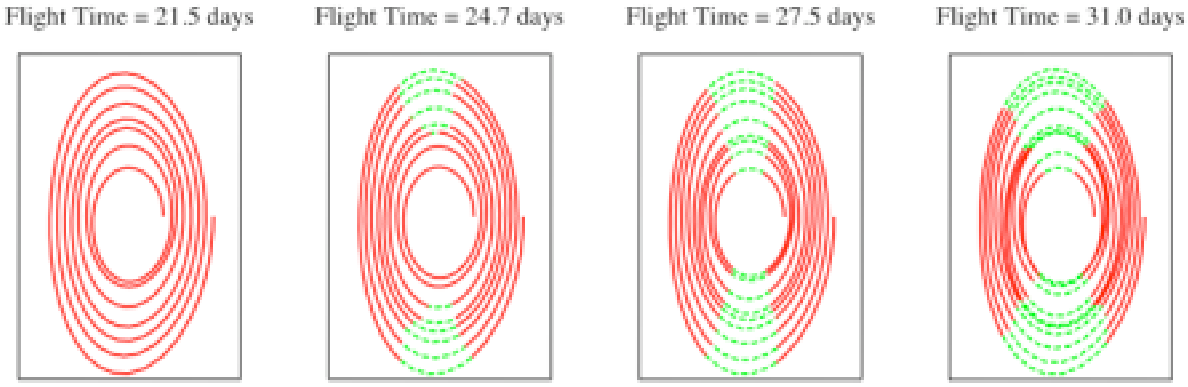

Figure 5. Pareto-optimal trajectories found with the present method for Problem II. The red solid and the green dashed lines represent thrusting and coasting arcs, respectively. As the flight time increases, several coast arcs are inserted around the y-axis.

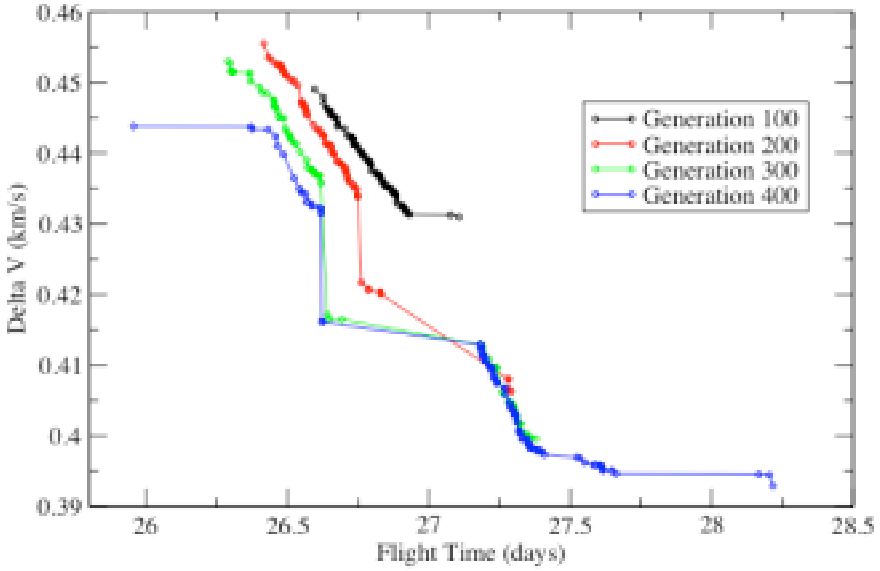

Figure 6. Pareto-optimal solutions found for Problem III. As the population evolves in the process of the genetic algorithm, the Pareto-optimal solutions improve in terms of both Pareto-optimality and the wide spread of the Pareto front.

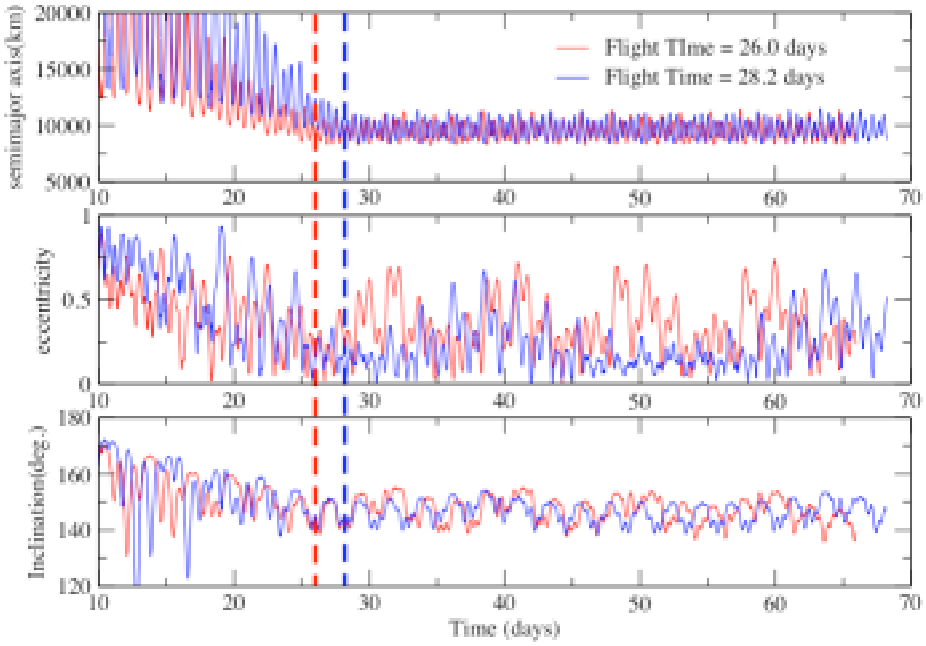

Figure 7. Orbit dynamics of two Pareto-optimal solutions found for Problem III. The trajectories are propagated without thrust for additional 40 days after reaching the target DRO state in order to monitor the stability of the final DRO state. Both trajectories remain stable. The vertical dashed lines indicate the flight time at which the orbit reaches the target and the thrust is turned off thereafter.

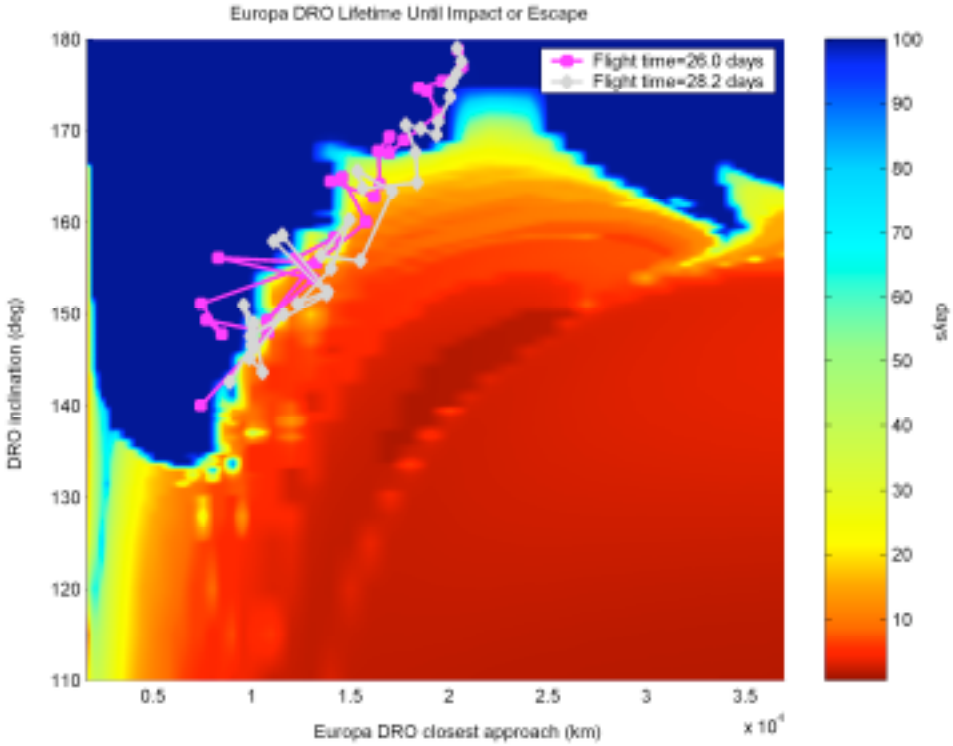

Figure 8. Stability map for distant retrograde motion in the Jupiter-Europa system. The color represents the time until impact or escape for DROs with specified initial closest approach and inclination. The paths of two Pareto optimal solutions from Problem III are shown.

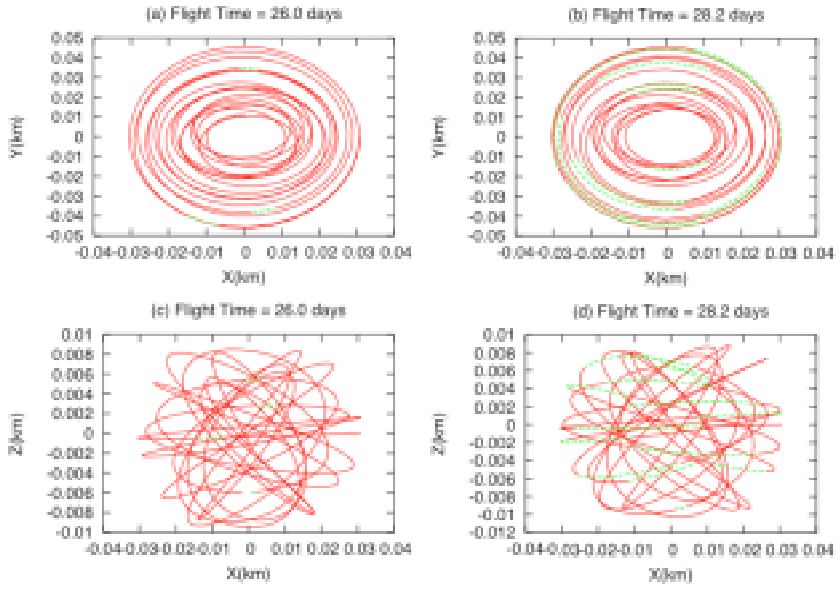

Figure 9. Top view (x-y plane) and side view (x-z plane) of trajectories of two Pareto-optimal solutions of Problem III. The coordinates of the trajectories are defined in the rotating frame.

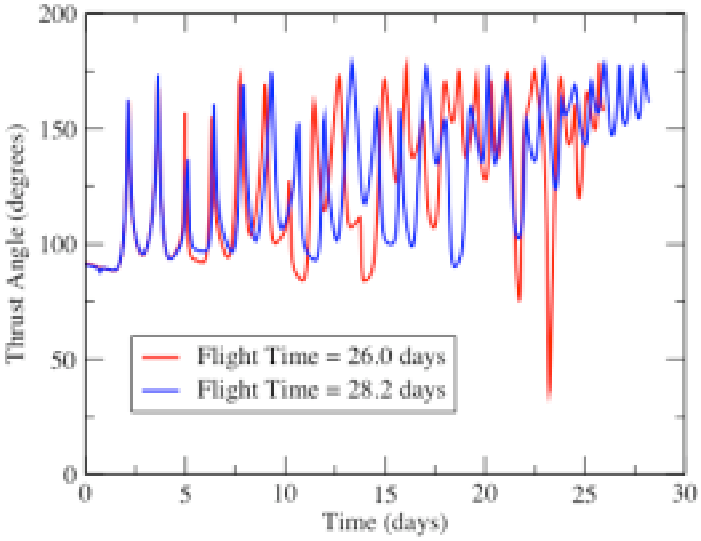

Figure 10. Thrust angles of two Pareto-optimal solutions of Problem III. The thrust angle is defined by the angle between the thrust vector and the spacecraft velocity vector in the rotating frame. When the thrust magnitude (Figure 11) is zero during coasts, the thrust angle is still defined according to the Primer Vector control law.

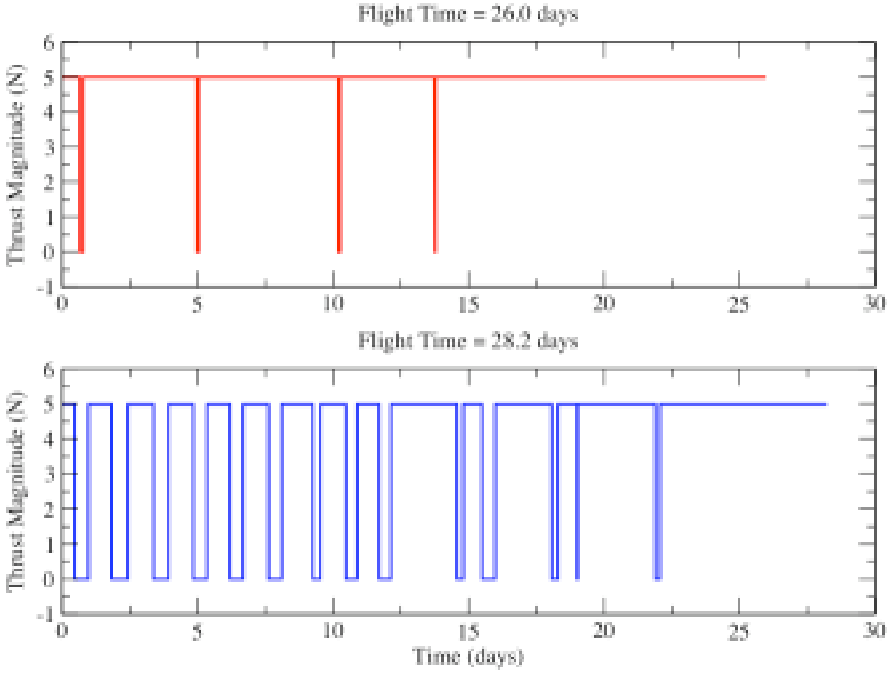

Figure 11. Thrust magnitudes of two Pareto-optimal solutions of Problem III. It has a "bang-bang" structure with the thrust magnitude of 4.98 N when thrusting. The solution with the flight time of 26 days has four very short coasting arcs, indicating that it is close to the shortest flight time solution.

REFERENCES

1. J.T. Betts, "Survey of Numerical Methods for Trajectory Optimization", *J. Guidance, Control, and Dynamics,* 21(2), 193-207, 1998.
2. F. Fletcher, Practical Methods of Optimization, John Willey & Sons, 2 edition, 2000.
3. Lawden, D. F., Optimal Trajectories For Space Navigation, Butterworths & Co. (Publishers) Ltd., Lon-don, 1963.
4. Marec, Jean-Pierre, Optimal Space Trajectories, Elsevier Scientific Publishing Company, Amsterdam, 1979.
5. Jezewski, D. J., "Primer Vector Theory and Applications," Technical Report NASA TR R-454, Lyndon B. Johnson Space Center, Houston, Texas, 77058, November 1975.
6. Russell, R.P., "Primer Vector Theory Applied to Global Low-Thrust Trade Studies," AAS 06-156, 16th AAS/AIAA Space Flight Mechanics Conference, Tampa, Florida, Jan. 22-26, 2005.
7. Goldberg, D.E., "Genetic Algorithms in Search, Optimization and Machine Learning", Addision-Wesley, 1989.
8. Metropolis, N., Rosenbluth, A.W., Rosenbluth, M.N., Teller, A.H., Teller, E., "Equation of State Calculation by Fast Computing Machines," *J. of Chem. Phys*. **21**, 1087-1091, 1953.
9. Eiben, A.E. and Smith J.E., "Introduction to Evolutionary Computing", Springer, 2003.
10. Reynolds, R.G., "An Introduction to Cultural Algorithms," Proceedings of the Third Annual Conference on Evolutionary Programming, p131-139, 1994.
11. A.E. Petropoulos, "Simple Control Laws for Low-Thrust Orbit Transfers," AAS 03-630, AAS/AIAA Astrodynamics Specialist Conference, Big Sky, Montana, Aug. 03-07, 2003.
12. A.E. Petropoulos, "Low-Thrust Orbit Transfers Using Candidate Lyapunov Functions with a Mechanism for Coasting," AIAA 04-5089, AIAA/AAS Astrodynamics Specialist Conference, Providence, Rhode Island, Aug. 16-19, 2004.
13. A.E. Petropoulos, "Refinements to the Q-Law for Low-Thrust Orbit Transfers," AAS 05-162, AAS/AIAA Space Flight Mechanics Conference, Copper Mountain, Colorado, Jan. 23-27, 2005.

14. B. Dachwald, "Evolutionary Neurocontrol: A Smart Method for Global Optimization of Low-Thrust Trajectories" AIAA 04-5405, AIAA/AAS Astrodynamics Specialist Conference, Providence, Rhode Island, Aug. 16-19, 2004.

15. S. Lee, P. von Allmen, W. Fink, A.E. Petropoulos, and R.J. Terrile, "Design and Optimization of Low-Thrust Orbit Transfers using the Q-law and Evolutionary Algorithms," IEEE Aerospace Conference Proceedings, Big Sky, Montana, Mar. 7-11, 2005.

16. S. Lee, P. von Allmen, W. Fink, A.E. Petropoulos, and R.J. Terrile, "Comparison of Multi-Objective Genetic Algorithms in Optimizing Q-Law Low-Thrust Orbit Transfers," GECCO Conference Late-breaking Paper, Washington, D.C., Jun. 25-29, 2005.

17. S. Lee and A. E. Petropoulos, "Low-Thrust Orbit Transfers Optimization with Refined Q-law and Multi-Objective Genetic Algorithms," AAS/AIAA Astrodynamics Specialist Conference, Lake Tahoe, Aug. 30- Sep. 1, 2005.

18. K. Deb, *Multi-Objective Optimization Using Evolutionary Algorithms,* John Wiley & Sons, 2001.

19. C.A.C. Coello, D.A. Van Veldhuizen, and G.B. Lamont, *Evolutionary Algorithms for Solving Multi-Objective Problems (Genetic Algorithms and Evolutionary Computation)*, Penum US, 2002.

20. K. Deb, A. Pratap, S. Agarwal, and T. Meyarivan, "A Fast and Elitist Multiobjective Genetic Algorithm: NSGA-II," *IEEE Transactions on Evolutionary Computation*, Vol. 6, 182-197, 2002.

21. M. Vasile, "A Global Approach to Optimal Space Trajectory Design," AAS 03-141, AAS/AIAA Space Flight Mechanics Meeting, Punce, Puerto Rico, 2003.

22. S. Rocca et al, "Optimal Low-Thrust Trajectory Analysis for Constant and Variable Specific Impulse Thrusters Generated by Multi-objective Evolutionary Algorithms and Nonlinear Programming," AAS/AIAA Space Flight Mechanics Conference, Maui, Hawaii, 2004.

23. B. Wall and B. A. Conway, "Near-Optimal Low-Thrust Earth-Mars Trajectories via a Genetic Algorithm," J. of Guidance, Contro, and Dynamics, Vol. 28, pp. 1027, 2005.

24. P. Rogata, E. D. Sotto, M. Graziano, F. Graziani, "Guess Value for Interplanetary Transfer Design Through Genetic Algorithms," AAS/AIAA Space Flight Mechanics Conference, Ponce, Puerto Rico, 2003.

25. J. Igarashi and D. B. Spencer, "Optimal Continuous Thrust Orbit Transfer Using Evolutionary Algorithms," J. of Guidance, Control, and Dynamics, Vol. 28, pp 547, 2005.

26. S. Lee, W. Fink, R. Russell, P. von Allmen, A. E. Petropoulos, and R. J. Terrile, AIAA 2005-6835 Paper, AIAA Space Conference, Long Beach, August 30- September 1, 2005.

27. S. Lee, R. P. Russell, W. Fink, R. J. Terrile, A. E. Petropoulos, and P. von Allmen, peer-reviewed and accepted for presentation in IEEE Aerospace Conference, Big Sky, Montana, March 4-11, 2006.

28. T. P. Runarsson and X. Yao, "Stochastic Ranking for Constrained Evolutionary Optimization," IEEE Transactions on Evolutionary Computation, Vol. 4, No. 3, 2000, pp. 284-294.

29. G. J. Whiffen and J. A. Sims, "Application of a Novel Optimal Control Algorithm to Low-Thrust Trajectory Optimization," AAS/AIAA Space Flight Mechanics Meeting, AAS Paper 01-209, Santa Barbara, California, Feb. 11-15, 2001.

30. G. J. Whiffen, "Optimal Low-Thrust Orbit Transfers around a Rotating Non-Spherical Body," AAS/AIAA Space Flight Mechanics Meeting, AAS Paper 04-264, Maui, Hawaii, Feb. 8-12, 2004.

31. Lam, T., Whiffen, G. J., "Exploration of Distant Retrograde Orbits around Europa," Paper AAS 05-110, 15th Spaceflight Mechanics Meetings, Copper Mountain, Colorado, January 2005.

32. Whiffen, G. J., "Jupiter Icy Moons Orbiter Reference Trajectory," Paper AAS 06-186, AAS/AIAA Space Flight Mechanics Meeting, Tampa, Florida, 2006.